Research Article

Nonlinear vibration of crowned gear pairs considering the effect of Hertzian contact stiffness

Moslem Molaie[1] · Farhad S. Samani[1,2] · Habibollah Motahar[1]

Abstract
This study aims to analyze the influence of lead crowning modification of teeth on the vibration behavior of a spur gear pair. Two dynamic rotational models including an uncrowned and crowned gear are examined. Hertzian mesh stiffness is computed using tooth contact analysis in quasi-static state along a complete mesh cycle of teeth mesh. The dynamic orbits of the system are observed using some useful attractors which expand our understanding about the influence of crown modification on the vibration behavior of the gear pair. Nonlinear impact damper consists of non-integer compliance exponents identify energy dissipation of the system beneath the surface layer. By augmenting tooth crown modification, the surface penetration increases and consequently normal pressure of the contact area becomes noticeable. Finally, the results show modification prevents gear pair to experience period doubling bifurcation as the numerical results proved. Using this new method in dynamic analysis of contact, broaden the new horizon in analyzing of the surface of bodies in contact.

Keywords Nonlinear vibration · Crowned gear · Hertzian contact · Finite element method

1 Introduction

Gear transmission systems are known as discontinues dynamical systems that transmit power and motion between shafts. During the transmission, mating gears have their own dynamic characteristics with one or more common points in local contact zones. Impact and friction complete the power transmission of system [1] which might be accompanied by repeated impacts called Vibro-impact process. Excessive noise and large dynamic load are striking features of Vibro-impact transmission systems which are in conflict with the demand for acoustic comfort especially in automotive industries. Tooth contact analysis (TCA) of gears paves the way of study on the nonlinear vibration of those systems by means of analytical and computational techniques.

A number of researches have been carried out on the influence of crown modification in the quasi-static state of the mesh stiffness, transmission error and deflection of gears and so on such as Refs. [2, 3]. Similarly, some papers studied the influence of geometric modification and fault on the dynamics of gears. An experimental study is presented by Gelman et al. [4] in order to test the performance of the wavelet spectral kurtosis techniques, which is a way to diagnose gear tooth fault early. Chen et al. [5] used experimental data, static transmission error and backlash, to investigate impact behavior of crowned gear in terms of the dynamic load factor. Again, impact damping was the major concern of the study by Li-juan [6] which considered nonlinear damping coefficient with integer and non-integer compliance exponents.

The total displacement of gears in mesh is a summation of some deformations such as deflection due to bending,

✉ Farhad S. Samani, farhad.samani@uk.ac.ir; Moslem Molaie, moslem_molaie@yahoo.com; Habibollah Motahar, Habibollahmotahar@yahoo.com | [1]Department of Mechanical Engineering, Shahid Bahonar University of Kerman, Kerman 76175-133, Iran. [2]Department of Engineering "Enzo Ferrari", University of Modena and Reggio Emilia, Via P. Vivarelli 10/1, 41125 Modena, Italy.

SN Applied Sciences (2019) 1:414 | https://doi.org/10.1007/s42452-019-0439-y

Received: 21 November 2018 / Accepted: 2 April 2019 / Published online: 5 April 2019

shear and surface indentation. Sánchez et al. [7] studied the mesh stiffness of spur gear pairs by considering the Hertzian effect and presented mesh stiffness equations approximately. To achieve the mesh stiffness, Sánchez considered some factors such as bending, shear, compressive and contact deflections. The presented equation determined the load sharing ratio and calculated the load at any point of the path of contact for spurs gears. Cheng et al. [8] determined the time-varying mesh stiffness with considering the effect of Hertzian deflection and different loads by means of finite element method. An analytical model is presented to calculate mesh stiffness by Ma et al. [9]. This study investigated the mesh stiffness for gear pairs with tip relief. It led to inhibition about overestimate the mesh stiffness during double-tooth contact and consideration of the tooth flexibility effects.

What makes this paper utterly different from the others is directly considering the effect of the Hertzian deflection on the dynamic gear behavior by entering into the dynamic equation. In order to use Hertzian contact damping and Hertzian contact restoring force accurately in dynamic equation of motion, it is necessary to separate surface penetration from other deflections of mesh in spite of making the complex model.

Any change in surface characteristics of mesh arises some changes in the contact pattern of bodies and consequent change in the vibration behavior of the system. Distinguishing the deflection of elements paves the way of study on contact fatigue [10] in dynamic state when the contacting stresses are repetitive at the surface points. Based on this issue, in the present study, the influence of Hertzian contact pattern on the dynamic transmission error of gear mesh has been located at the center of attention to show the effects of crown modification on the nonlinear behavior of the system, comparing crowned gear with uncrowned one. Thanks to the "*HelicalPair*" software [11, 12] developed in the Center Intermech MO.RE. (Aster, High Technology Network of the Emilia Romagna Region) which enabled us to generate deformable models with different amplitudes of crowning. It should be mentioned that "*Helicalpair*" has been widely used in the recent studies and the correctness of the results has been proved in Refs. [12–15].

Moreover, equivalent stiffness of the present gear pair consists of two terms. The first term possess the bending flexibility of the teeth and also flexibility of the gear web and hub. The second term is the flexibility of the Hertzian contact deformation. Each of these two terms behaves as a spring with time dependent stiffness. In this paper the portion of total stiffness for Hertzian contact deformation analyzed separately and its effectiveness illustrated clearly. Finally, the nonlinear dynamics of the gear pair considering the equivalent stiffness is presented.

2 Physical model

In order to model the dynamic behavior of a spur gear pair, usually a model is presented, including important elements on the dynamics of pairs such as mesh stiffness, viscous damping, equivalent mass and backlash [13]. A new equivalent model, including all typical elements has been shown in Fig. 1, but it has a subtle difference with ordinary models. A time varying stiffness shown as k_h has been connected to a time varying stiffness k serially. k_h and k are the coefficients associated with the springs and replaced as the Hertzian mesh stiffness and remained mesh stiffness respectively. This is a novel model of connection of two nonlinear springs in gear study. Ref. [16] studied on this type of serial connection to investigate the natural frequency and dynamic response of such nonlinear system thoroughly. The governing equations of motion of the system shown in Fig. 1 are given by Eq. 1:

$$\begin{cases} \ddot{x} + \frac{kr_1^2}{I_1}\left(f(x) - \delta_h\right) + \frac{k_h r_2^2}{I_2} g(\delta) + \frac{cr_1^2}{I_1}\left(\dot{x} - \dot{\delta}_h\right) + \frac{Dr_2^2}{I_2}\dot{\delta}_h g(\delta) = T_e \\ k\left(f(x) - \delta_h\right) + c\left(\dot{x} - \dot{\delta}_h\right) - k_h g(\delta) - D\dot{\delta}_h g(\delta) = 0 \end{cases} \tag{1}$$

The second part of Eq. 1 obtained from the equilibrium point between springs and dampers. δ_h corresponds the net displacements of the spring associated with k_h which shows dynamic penetration of tooth surfaces

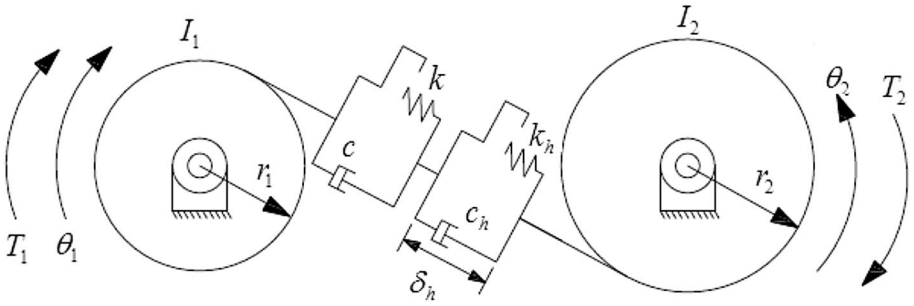

Fig. 1 The physical model including Hertzian mesh stiffness and damping Ref. [14]

in contact and x is the dynamic transmission error of the system (displacement of equivalent mass) where $x(t) = r_1\theta_1(t) - r_2\theta_2(t)$. $\theta_1(t)$ is the angular position of the driver wheel (pinion), $\theta_2(t)$ is the angular position of the driven wheel (gear); r_1 and r_2 are based radii; b_c is half of the backlash due to operating center distance modification along the line of action, c is constant viscous damping and c_h denotes Hertzian damping; I_1 and I_2 are the rotary inertia of pinion and gear respectively. $k(t)$ and $k_h(t)$ are time varying mesh stiffness and Hertzian stiffness, respectively. Notice that $k(t)$ does not cover Hertzian mesh stiffness and $T_e = T_1 r_1/I_1 + T_2 r_2/I_2$. T_1 and T_2 are applied torques on pinion and gear, respectively.

The dots $(\cdot)$ over letters denote the derivation with respect to time. It is important to consider a function for surface penetration (SP), so $g(\delta)$ is defined in Eq. 3. The Backlash function in Eq. 2 [13] confines displacement in backlash vicinity. Therefore, there are zero values for $g(\delta)$ and $f(x)$ when tooth locates between adjacent teeth $-b < x < b$, means contact loss. It is obvious that both functions $f(x)$ and $g(\delta)$ are in the same phase.

$$f(x) = \begin{cases} x - b_c, & x \geq b_c \\ 0, & -b_c < x < b_c \\ x + b_c, & x \leq -b_c \end{cases} \tag{2}$$

$$g(\delta) = \begin{cases} \delta^n, & x \geq b_c \\ 0, & -b_c < x < b_c \\ -\delta^n, & x \leq -b_c \end{cases} \tag{3}$$

In addition, in forward motion when $x \geq b_c$, the surface penetration grows by exponent $n = 3/2$ for crowned teeth and $n = 1$ for uncrowned teeth [17].

The term $k_h g(\delta) + D\dot{\delta} g(\delta)$ in Eq. 1 illustrates gear impact force of the model where $D = \mu\delta^n$ is the damping coefficient [17]. Hunt and Crossley introduced $\mu = \frac{3}{2}\alpha k$ [18] where $\alpha = (1 - e)/v_i$ has a value between 0.08 and 0.32 s/m based on experimental data for steel. In this study, 0.26 s/m has been assumed for α and the mean value k_{mh} of Hertzian mesh stiffness has been replaced for k, which will discuss in the next section completely. e is defined as the ratio of relative speeds after and before an impact along the common normal of surfaces in contact of colliding teeth; coefficient of restitution along the line of action. The term k_h is taken into account as time-varying functions implementing Fourier series by fundamental meshing frequency $\omega_m = \frac{2\pi}{60} N_1 \gamma_s$, see Eq. 4. N_1 is the teeth number of pinion and γ_s(rpm) is the input shaft speed. The approximation of the mesh stiffness is expanded by a Fourier expansion, which is obtained numerically using

Table 1 Numerical parameters of the gear pairs

Parameters	Pinion	Gear
Number of teeth	23	34
Module (mm)	3	3
Pressure angle (°)	20	20
Face width (mm)	20	20
Module of elasticity (MPa)	206,000	206,000
Poisson ratio	0.3	0.3
Density (kg/m^3)	7850	7850
Contact ratio	1.559	
Backlash	0.1172	
Viscous damping coefficient	0.015	

"*HelicalPair*" software and *MSC Marc* simultaneously. Table 1 consists of the design parameters of the gear pair thoroughly.

$$k_h(t) = k_{mh} + k_{hj} \sum_{j=1}^{s} \cos(j\omega_m t - \varphi_j) \tag{4}$$

In Eq. (4), k_{mh} is the average value of torsional Hertzian stiffness. Amplitudes k_{hj} and phases φ_j are obtained from the discrete Fourier transform for $S = 9$ samples, discrete rotational position over a mesh cycle. Notice that, in order to decrease nonlinearity of the Eq. 1, the time varying pattern of k has been neglected by considering the average value of corresponding stiffness, using Fourier transform. For unmodified tooth $k = 4.17 \times 10^5$ N/mm and for crowned pair $k = 2.79 \times 10^5$ N/mm. The dynamic model employs a number of assumptions. First of all, there is no friction such as sliding friction in the dynamic model as the study of Refs. [19, 20]. The gears are considered perfectly rigid with flexibility of mesh and surface and no mounting errors and misalignment are included. The tooth profile for both models is perfectly involute. The surfaces are continuous and non-conforming [21].

3 Computing Hertzian mesh stiffness of contact

There are some studies investigated mesh stiffness of gear pairs by means of experimental equipment such as Ref. [22], or by numerical techniques as Ref. [11] and analytical approaches like Ref. [23]. Here, the key point of computation of stiffness is based on the Hertz theory with the localized bearing contact of mating teeth in single contact and double contact points during a mesh cycle. The surface assumed frictionless along finite element (FE) analysis and the contact area is much smaller than the characteristic

dimensions of the contacting bodies. At unloaded surface of contact, two principal radii of curvature are assumed for each pair on the corresponding principal plane of curvature ($\sum 1$ and $\sum 2$). Two of those radii are radius of curvature of involute profile [24] named R_{ij} on $\sum 1$ plane, where $i = 1, 2$ for pinion and gear respectively and j demonstrates the tooth number in contact. The second category of radius of curvature ρ_{ij} is perpendicular to the first type on $\sum 2$ plane. Note that the corresponding principal curvatures are perpendicular because no misalignment is deemed, as in Fig. 2 is shown. This radius of curvature presents lead to crown modification of the tooth geometry which is calculable by means of simple mathematical formula [2].

When there is no lead crowning modification on teeth, i.e., $\beta = 0$ and $\rho_{ij} = \infty$ the contact area is rectangular, while two crowned teeth make an elliptical contact area. Theoretically, the shape of the contact can be defined with two dimensions, major semi-axis, a, and minor semi-axis, b, (Ref. [21]) as shown in Fig. 3. Having both semi-axis and using Hertz solution enabled us to calculate approximately static compression of contact area. Equation 5 consists of geometrical values a and b, [21, 25], material property E and transmitted load between the pair of teeth.

$$\delta = \frac{3}{2}\frac{F}{\pi ab}\frac{1}{E^*}bk(e) \tag{5}$$

where $k(e) = \int_0^1 \left(1 - t^2\right)\left(1 - et^2\right)^{-0.5} dt$, the complete elliptical integral of the first kind that depends on the eccentricity of the ellipse, $e = \sqrt{1 - b^2/a^2}$. $E^* = \left(\frac{1-\upsilon_1^2}{E_1} + \frac{1-\upsilon_2^2}{E_2}\right)^{-1}$ is the equivalent elastic modulus based on elastic modules E_1 and E_2 and the Poisson ratios ν_1 and ν_2 of pinion and gear, respectively. Transmitted loads on each tooth are time varying due to changes in contact

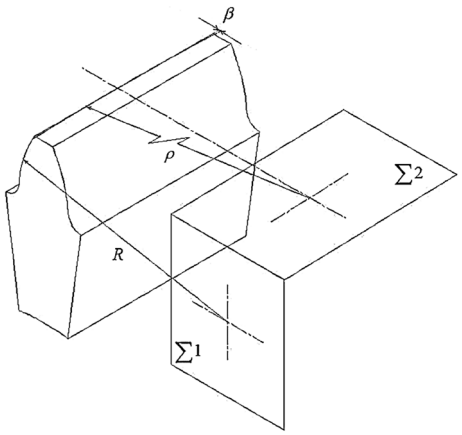

Fig. 2 Two perpendicular planes of curvatures, β is the amplitude of crowning

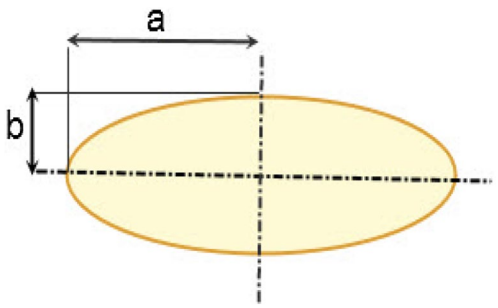

Fig. 3 Two dimensions of contact area

position between single and double teeth during a mesh cycle; see Fig. 4. Tooth contact analysis (TCA) is begun when pitch points of both driver and driven gear are matched. In this situation, the greatest portion of the load is shared between teeth and for crowned tooth; it leaves an elliptical area as Fig. 5. The rotation continues to the start point of double tooth contact at ε (the time of start of double involvement) Fig. 4, the highest point of single tooth contact (HPSTC).

Obviously, the contact area $A_c = \pi ab$ and compression δ during this period have the highest amount as TCA proved. Then continues through c-1 (the duration of double tooth contact) to reach to the lowest point of single tooth contact (LPSTC), c is the contact ratio, see Table 1. A_c seems to be lower than the previous segment because of division of the transmitted load between two pair of teeth in contact. Consequently, lower compression appears. Finally, the mating teeth experience the second single tooth contact duration, during the

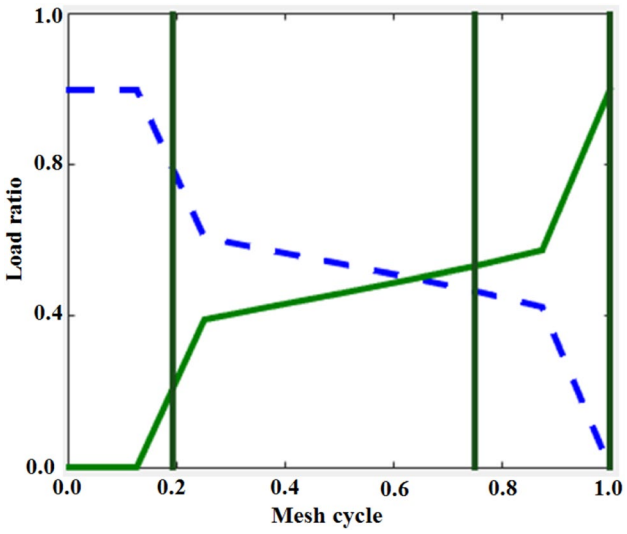

Fig. 4 Proportion of applied transmitted load on mating teeth during one mesh cycle, - - - the first tooth, —— the following tooth

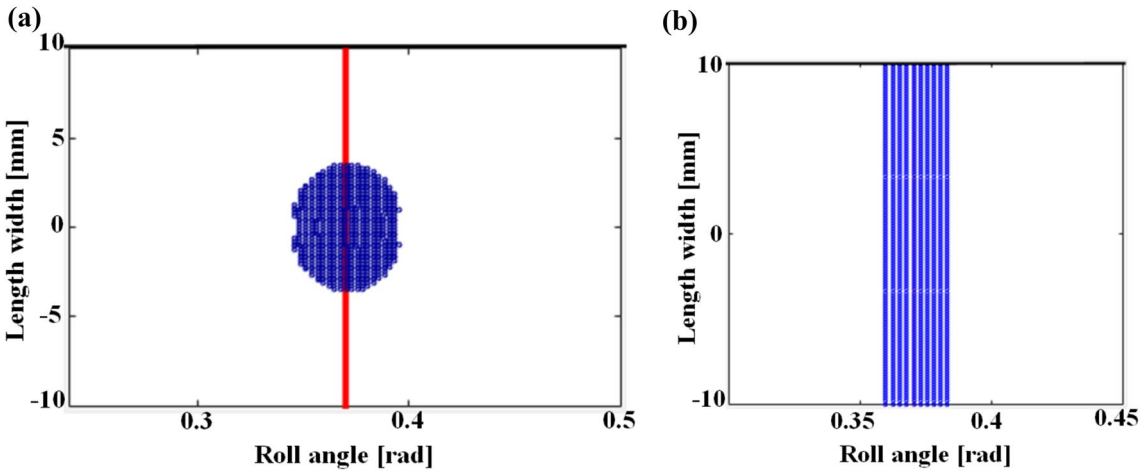

Fig. 5 Determination of the first contact position shape, **a** crowned teeth, **b** uncrowned teeth

remained time, $2-(c-\varepsilon)$. ε is calculable if the approach and recession length of contact line be accessible.

By means of Eq. 5, the *maximum surface penetration* would be attainable for each contact position. The relation between applied normal contact force and relative displacement of the two surfaces is given by Eq. 6. For elliptical shape [21], it would be a nonlinear equation with exponent $n = 3/2$, whereas for rectangular contact $n = 1$ [26].

$$F = k_h \delta^n \tag{6}$$

$k_h\left(\mathrm{N/mm}^{\frac{3}{2}}\right)$ demonstrates Hertzian mesh stiffness in contact [17] with a nonlinear relation with maximum surface penetration and load. Figure 6 depicts the time varying Hertzian mesh stiffness from Fourier transform output for two models through a mesh cycle.

Comparison of Fig. 6a, b reveals that by lead crowning modification, a small change appears in contact pattern and remarkable change in stiffness which is the consequence of different approach toward penetration (using different exponents).

To clarify the magnitude of the Hertzian mesh stiffness for the considered gear mesh, the equivalent Hertzian mesh stiffness estimated by means of Eq. 6. Moreover, the total mesh stiffness is evaluated using "*Helicalpair*" software and *MSC Marc* commercial finite element code. Figure 7 shows the comparison of the Hertzian mesh stiffness and total mesh stiffness for the considered spur gear with uncrowned teeth.

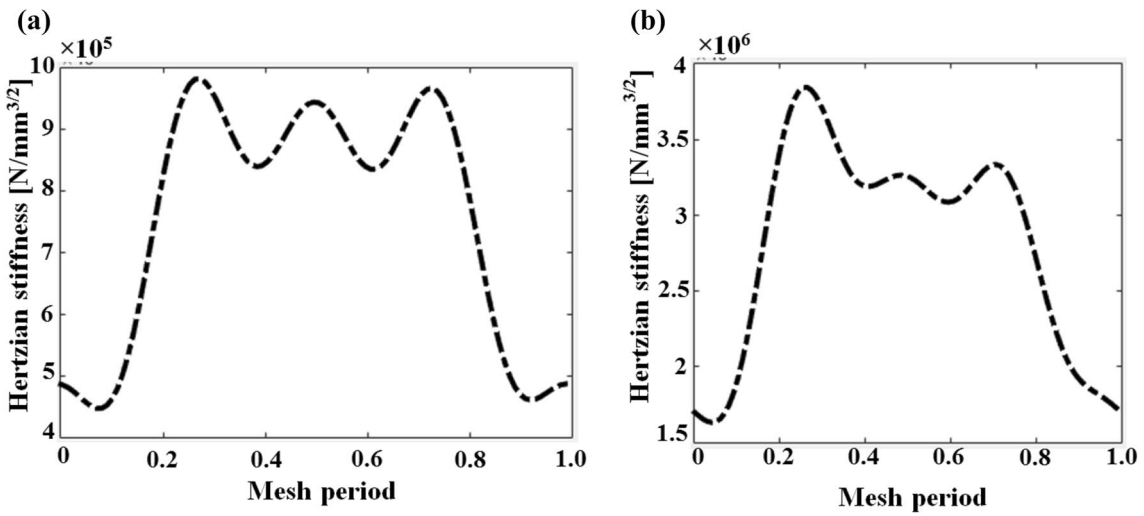

Fig. 6 Hertzian mesh stiffness of two cases, **a** crowned teeth, **b** uncrowned teeth

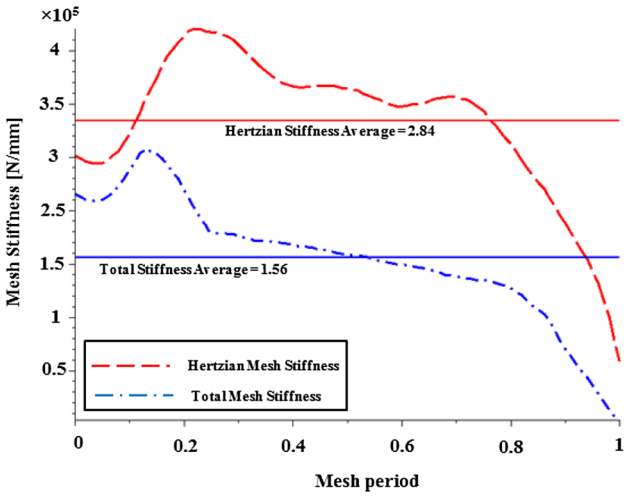

Fig. 7 Comparing between Hertzian mesh stiffness and total mesh stiffness for uncrowned teeth

4 Dynamic analysis of modified and unmodified gears

The two degree-of-freedom equation of motion illustrated in Eq. (1) solved by means of a numerical integration based on fourth order Runge–Kutta integration routine by taking into account initial conditions of $x(0) = 1.0001b_c$, $\dot{x}(0) = 0.001b_c$, $\delta(0) = 9.89 \times 10^{-4}b_c$. In order to calculate the initial compression of teeth surface, static force equilibrium of serial springs is considered employing $f(x) = \delta + \eta\delta^{\frac{3}{2}}$ where $\eta = k_{mh}/k$. The computation is started when teeth are in a weakly touch with a very slight surface compression. Two cases are studied in the present manuscript, see Table 2, in order to gain deeper insight into the influence of tooth modification on the dynamic behavior of the models. The pinion is assumed to excite system with the low speed of 150 (rpm) and 210,000 (N mm) torque load along 800 mesh periods including 100 sampling points in each period.

In this study, a numerical attempt has been done in order to investigate the tooth separation and impact phenomenon. Surprisingly, both models suffer from successive separations through simulation. In a complete contact loss duration, the equation of motion (1) reduced to $\ddot{x} = T_e$, when all restoring forces and the dissipative terms become zero. Figure 8a, b show the time history of dynamic responses of two models over the steady state mesh periods. Dynamic Transmission Error (DTE) and the Surface Penetration (SP) for unmodified model and the modified model are also presented in these figures. In order to demonstrate quantitatively the results in each figure, DTE and SP have been figured simultaneously. Note that the distance between vertical black lines shows a sample of excitation period (internal excitation period, T_m) [19]. Vertical black line shows the system fluctuate longer than internal excitation. Crossing the DTE line through the backlash line means the onset of losing contact.

Root-mean-squares (the square root of the arithmetic mean of the squares of a set of responses) of both cases reveal that the unmodified gear pair with 149 μm endures much more deflection than the modified gear pair with 85.5 μm, akin to its static deflection of finite element modeling (FEM). Likewise, the surface penetration of the second model is deflected 5.5 times than the first one. Moreover, while the fluctuation of modified gear pair (match with an excitation fluctuation period) is rather substantial and reflects two contact losses, the unmodified gear pair fluctuates in lower amplitude but meets six contact loss along a period of its fluctuation.

Through an arbitrary period of excitation, the first separation emerges along double tooth contact (DTC) for both cases. However, unmodified gear sees two successive contact losses along DTC before the second static tooth contact (STC2) while modifying pair experience one separation over DTC and one over STC2 (Fig. 9). The

Table 2 Parameters of gear system

Model	Crown amplitude β (mm)	Compliance exponent n
Uncrowned	0	1
Crowned	0.08	1.5

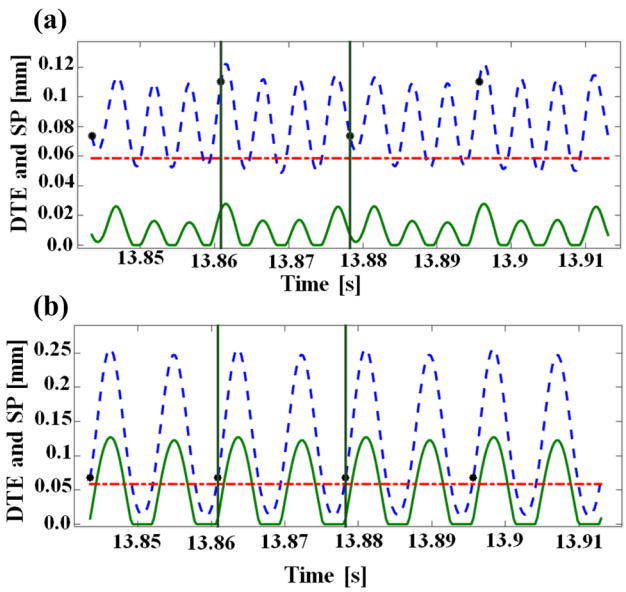

Fig. 8 Steady state time responses, **a** crowned teeth, **b** uncrowned teeth, - - - DTE, —— SP, -·-·- backlash magnitude, • mesh period indicators

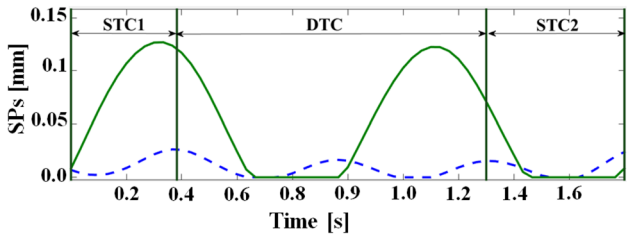

Fig. 9 Time history along a mesh period of SPs in different contact types. *DTC* double tooth contact, *STC* single tooth contact, —— crowned teeth, - - - uncrowned teeth

duration of contact loss in the unmodified model is much more than the duration for modified pair. It seems that the impact's durations are not instantaneous for the modified model because 30% of the mesh cycle sees contact loss with identical time span which is a long duration. The accurate location of DTC and STCs are predictable because of the exact knowledge of the total time of the solution, sampling points during a mesh period and the length of a period for each simulation.

The system of modified model fluctuates with excitation period, time frequency T_m, period-1 motion (the motion repeats itself exactly every period of the external drive) through a mesh cycle in the steady state condition, see Fig. 10a. Amazingly, the uncrowned teeth model which has no modification on its teeth has much more potential to experience chaos as the Poincaré map observes period-2 motion (motion repeats itself exactly every two periods of the external drive) during the mentioned period, see Fig. 10b.

When teeth meet each other after separation, the amount of contact force rapidly increases and reaches to the maximum amount; see Fig. 11a, b. Interestingly, the mean value of dynamic Hertzian forces for both models are close together with 6.81 and 6.43 kN for uncrowned and crowned pairs. Evidently, the normal pressure and maximum shear stress of contact area follow this pattern consequently. Furthermore, it is reasonable to expect that due to the crowning and decreasing the area of contact, the contact normal pressure for the crowned teeth case must be much more than uncrowned teeth case. In this

Fig. 10 Poincaré map of oscillators in 150 rpm, **a** crowned teeth, **b** uncrowned teeth

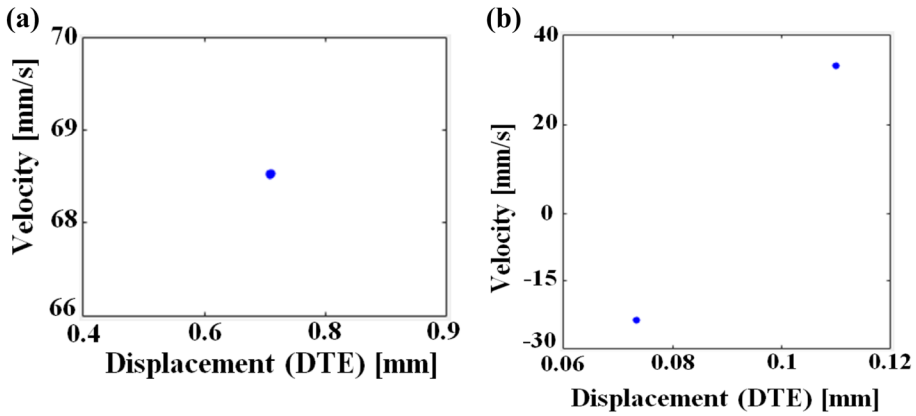

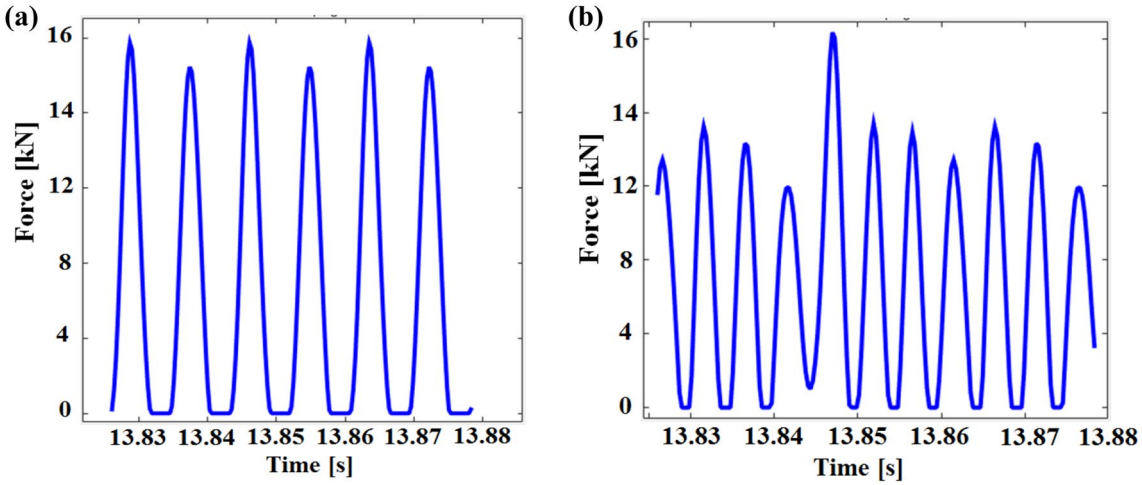

Fig. 11 Hertzian dynamic force of the models, **a** crowned teeth, **b** uncrowned teeth

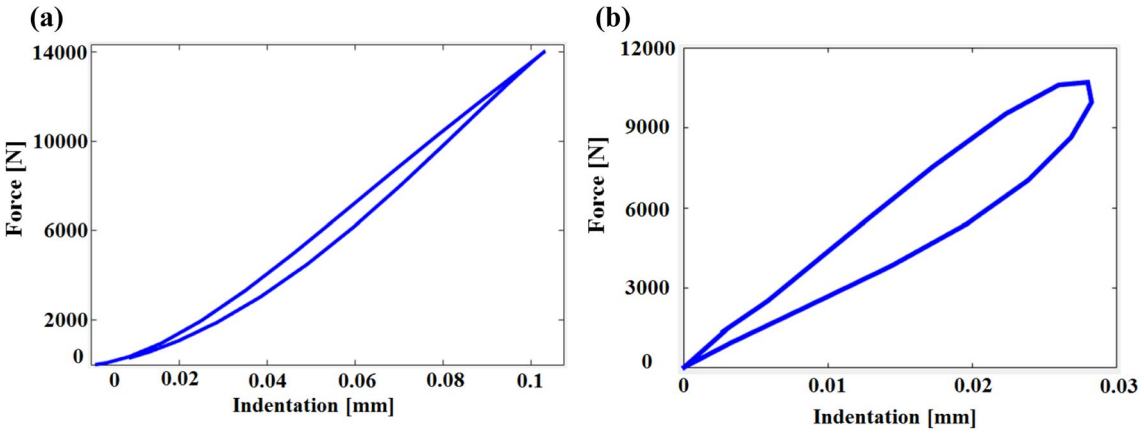

Fig. 12 Force–displacement map for $\alpha = 0.26$ s/m, **a** crowned teeth, **b** uncrowned teeth

simulation, exclusively forward contact and contact loss are visiting while in some cases, the impact occurs on the non-active flanks of a mating teeth pair. When a backside contact occurs at the line of action, it changes the motion direction instantaneously, see Ref. [14].

In gear rattling simulation, when the impact occurs, dissipated energy plays a significant role in the analysis. Hunt and Crossley [18] have shown force–displacement of Hertzian contacts which was satisfying for general mechanical contacts. Owing to the nonlinear nature of the contact force with the interaction of displacement, a closed loop is achieved; see Fig. 12a, b. In these figures the inner areas of the circuits illustrate energy dissipation due to collisions along a mesh cycle. There is one loop for each separation; however, for clear demonstration, the force–displacement of the first collision of each case has been plotted. It is noticeable, the nonlinear and linear trend of Fig. 12a, b respectively; which germane to the nonlinear and linear nature of the force–displacement equations. Figure 12b shows the characteristic curve of restoring force versus displacement as a straight line. However, crowned teeth model, Fig. 12a do not exhibit such a linear characteristic. It exhibits a characteristic such that the restoring force increases more rapidly than the displacement, called hardening nonlinearity.

There are closed loops for each contact loss or impact. Note that the amounts of dissipated energy are different as the initial velocity of contact for each meeting might be different.

5 Conclusion

Understanding the dynamic behavior of surface penetration assists us to be away from tooth health threatening phenomena such as contact resonance and heavy dynamic loads which lead detrimental effects on teeth surfaces. The result of this manuscript would be listed as follow:

- This paper defines the factors which produce the spur gear mesh stiffness. The effect of Hertzian mesh stiffness and tooth bending mesh stiffness are presented.
- The Hertzian dynamic force and possible teeth separation are presented for the spur gears with crowned and uncrowned teeth.
- Surface penetration for the dynamic loads is illustrated. Be means of this result, the portion of dynamic transmission error due to Hertzian surface deformation is specified.

Acknowledgements The authors would like to thank the Lab SIMECH/INTERMECH MO.RE. (HIMECH District, Emilia Romagna Region) particularly Prof. Francesco Pellicano and Dr. Marco Barbieri for providing "*HelicalPair*" software.

Compliance with ethical standards

Conflict of interest The authors declare that they have no conflict of interest to this work.

References

1. Luo AC, Guo Y (2012) Vibro-impact dynamics. Wiley, Hoboken
2. Li S (2015) Effects of misalignment error, tooth modifications and transmitted torque on tooth engagements of a pair of spur gears. Mech Mach Theory 83:125–136
3. Gurumani R, Shanmugam S (2011) Modeling and contact analysis of crowned spur gear teeth. Eng Mech 18(1):65–78
4. Gelman L, Chandra NH, Kurosz R, Pellicano F, Barbieri M, Zippo A (2016) Novel spectral kurtosis technology for adaptive vibration condition monitoring of multi-stage gearboxes. Insight-Non-Destr Test Cond Monit 58(8):409–416

5. Siyu C, Jinyuan T, Lijuan W (2014) Dynamic analysis of crowned gear transmission systen with impact damping: based on experimental transmission error. Mech Mach Theory 74:254–269
6. Wu LJ, Tang JY, Chen SY (2014) Effect of nonlinear impact damping with non-integer compliance exponent on gear dynamic characteristics. J Cent South Univ 21:3713–3721
7. Sánchez MB, Pleguezuelos M, Pedrero JI (2017) Approximate equations for the meshing stiffness and the load sharing ratio of spur gears including hertzian effects. Mech Mach Theory 109:231–249
8. Ma H, Zeng J, Feng R, Pang X, Wen B (2016) An improved analytical method for mesh stiffness calculation of spur gears with tip relief. Mech Mach Theory 98:64–80
9. Cheng Q, Shao Y, Liu J, Yin L, Du M, Yang Y (2017) Calculation of time-varying mesh stiffness affected by load based on FEM. In: ASME 2017 international design engineering technical conferences and computers and information in engineering conference, pp V010T11A010–V010T11A010
10. Glaese W, Shaffer S Contact fatigue, battelle laboratories. ASM Handbook, Fatigue and Fracture 19, 331–336
11. Barbieri M, Zippo A, Pellicano F (2014) Adaptive grid-size finite element modeling of helical gear pairs. Mech Mach Theory 82:17–32
12. Motahar H, Samani F, Molaie M (2015) Nonlinear vibration of the bevel gear with teeth profile modification. Nonlinear Dyn 83(4):1875–1884. https://doi.org/10.1007/s11071-015-2452-z
13. Faggioni M, Samani FS, Bertacchi G, Pellicano F (2011) Dynamic optimization of spur gears. Mech Mach Theory 46(4):544–557
14. Bonori G (2006) Static and dynamic modeling of gear transmission error. Ph.D. Thesis, University of Modena and Reggio Emilia
15. Bonori G, Barbieri M, Pellicano F (2008) Optimum profile modifications of spur gears by means of genetic algorithms. J Sound Vib 313(3):603–616
16. Tellı S, Kopmaz O (2006) Free vibrations of a mass grounded by linear and nonlinear springs in series. J Sound Vib 289(4):689–710
17. Lankarani HM, Nikravesh PE (1994) Continuous contact force models for impact analysis in multibody systems. J Sound Vib 5(2):193–207
18. Hunt KH, Crossley FRE (1975) Coefficient of restitution interpreted as damping in vibroimpact. Int J Appl Mech 42(2):440–445
19. Kahraman A, Singh R (1990) Non-linear dynamics of a spur gear pair. J Sound Vib 142(1):49–75
20. Liu G, Robert GP (2009) Impact of tooth friction and its bending effect on gear dynamics. J Sound Vib 320(4):1039–1063
21. Tesfahunegn YA, Rosa F, Gorla C (2010) The effects of the shape of tooth profile modifications on the transmission error, bending, and contact stress of spur gears. Proc Inst Mech Eng Part C J Mech Eng Sci 224(8):1749–1758
22. Li S (2007) Effects of machining errors, assembly errors and tooth modifications on loading capacity, load-sharing ratio and transmission error of a pair of spur gears. Mech Mach Theory 42(6):698–726
23. Tavakoli M, Houser D (1986) Optimum profile modifications for the minimization of static transmission errors of spur gears. J Mech Transm Autom Des 108(1):86–94
24. Litvin FL, Fuentes A (2004) Gear geometry and applied theory. Cambridge University Press, Cambridge
25. Gonzalez-Perez I, Iserte JL, Fuentes A (2011) Implementation of Hertz theory and validation of a finite element model for stress analysis of gear drives with localized bearing contact. Mech Mach Theory 46(6):765–783
26. Machado M, Moreira P, Flores P, Lankarani HM (2012) Compliant contact force models in multibody dynamics: evolution of the Hertz contact theory. Mech Mach Theory 53:99–121